Series of Quantum Finite Potential Wells as an Energy State Approximation of Solids

Beniam Kumela

August 2024

1 Abstract

In this paper, we use a series of finite quantum potential wells to approximate the energy states of a solid. First, we review common analytic and numerical solutions to the single potential well problem. Then, we generalize the numerical approach to the multi-potential well problem. Finally, we analyze results from all 2 problems and relate them to physical phenomena. Note any graphs plotted are highlighted in the corresponding Mathematica notebook submitted with this paper.

2 Single Finite Potential Well

We begin by defining the finite potential well problem. This is when a particle is confined to a "box" with finite potential walls. Classically, if the total energy of the particle is less than the potential energy barrier of the walls, it can't be found outside of the box. However, there is a non-zero probability of the particle being found outside of the box due to the quantum tunneling effect. This potential can be described by the expression and schematic below.

$$V(x) = \begin{cases} V_0 & \text{if } x < -\frac{L}{2} \\ 0 & \text{if } -\frac{L}{2} \leq x \leq \frac{L}{2} \\ V_0 & \text{if } x > \frac{L}{2} \end{cases}$$

Where L_x is the length of the well and V_0 is the depth of the well. This is defined and plotted in Mathematica as shown below.

We use this potential to solve the time-independent

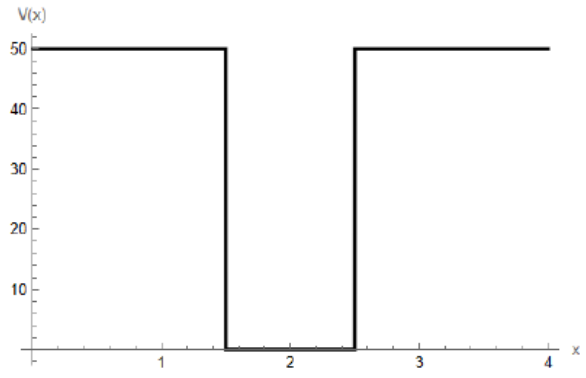

Figure 1: The finite potential well defined above where $L_x = 1$, $V_0 = 50$, and centered at x = 2.

Schrodinger's equation (TISE) for a quantized energy state, E, as shown below.

$$\frac{d^2\psi}{dx^2} = -\frac{2m}{\hbar^2}(E - V(x))\psi(x)$$

The general solution for this second order differential equation is given below for inside (V0=0) and outside (V0¿0) the well, respectively.

$$\frac{d^2\psi}{dx^2} = -k^2\psi \quad \Rightarrow \quad k = \sqrt{E + V_0}$$

$$\frac{d^2\psi}{dx^2} = l\psi \quad \Rightarrow \quad l = \sqrt{-E}$$

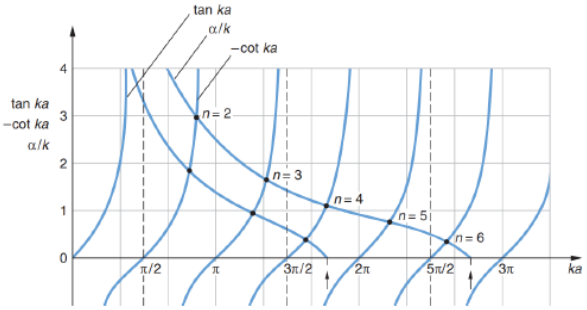

Figure 2: Example of graphical solutions from some form of Eqns. 9-10 to determine allowed energy states (UCSD, n.d.)

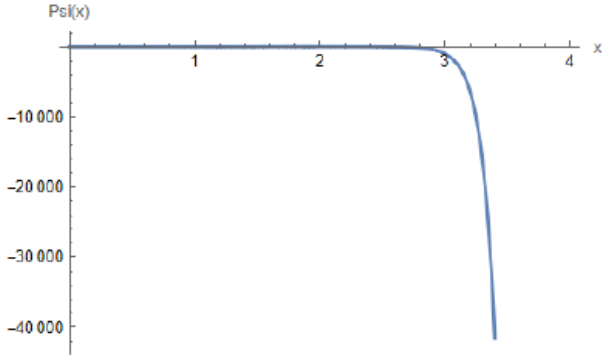

Figure 3: Wavefunction plotted as a function of position for E = 5.

$$\psi_{\text{even}}(x) = \begin{cases} Ae^{lx} & x < -\frac{L}{2} \\ D\cos(kx) & -\frac{L}{2} \leq x \leq \frac{L}{2} \\ Ae^{-lx} & x > \frac{L}{2} \end{cases}$$

$$\psi_{\text{odd}}(x) = \begin{cases} Ae^{lx} & x < -\frac{L}{2} \\ C\sin(kx) & -\frac{L}{2} \leq x \leq \frac{L}{2} \\ Ae^{-lx} & x > \frac{L}{2} \end{cases}$$

When enforcing the two boundary conditions, we solve the following expressions for Eqns. 5-6, respectively.

$$D\cos(-k) = Ae^{-l}, \quad kD\sin(k) = Ale^{-l}$$

$$Ae^{-l} = -C\sin(k), \quad Ale^{-l} = kC\cos(k)$$

We can now solve Eqns. 3-4 and 7-8 simultaneously for our desired energy as shown.

$$\sqrt{-E} = \sqrt{E + V_0}\tan(\sqrt{E + V_0})$$

$$-\sqrt{E + V_0}\cot(\sqrt{E + V_0}) = \sqrt{-E}$$

Eqns. 9-10 are usually graphed to corresponding energy states as shown below.

However, analytic solutions of the TISE are cumbersome or impossible to solve, especially for the higher dimensional systems we pursue later. We will stick with numerical methods, which scale better. Before we start we need to discretize the TISE using the finite-difference method as shown below starting from Eqn. 2.

$$\frac{1}{dx}\left(\psi(x + dx) - \psi(x)\right)dx - \psi(x) - \psi(x - dx)dx = -\frac{2m}{\hbar^2}(E - V(x))\psi(x)$$

For simplification we can define the function, f(x), as the following.

$$f(x) = -\frac{2m}{\hbar^2}(E - V(x))$$

$$\psi(x + dx) = dx^2 f(x)\psi(x) + 2\psi(x) - \psi(x - dx)$$

Finally, we can rewrite the expression in an iterative format.

$$\psi_{n+1} = (dx^2 f(x) + 2)\psi_n - \psi_{n-1}$$

This is done using Mathematica's NDSolve[] function, but let's show how such commerical solvers work by solving equations in an iterative fashion (Vetterling, 1998). This is solved below using the potential defined by Fig. 1, E = 5, m = 1, and h = 1.

This is not exactly what we would predict. The wavefunction should exponentially decay in the forbidden region but instead it blows up exponentially.

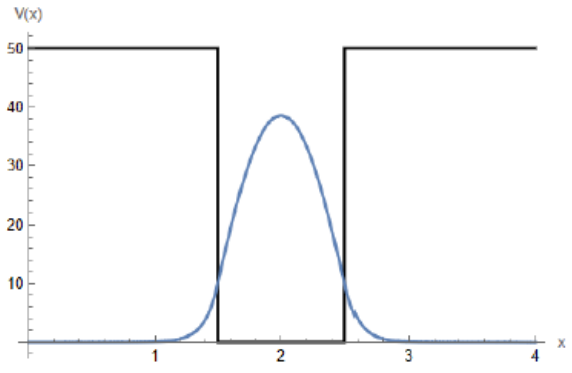

Figure 4: Corrected wavefunction (blue) plotted as a function of position and overlay with potential function (black) for E = 3.413571.

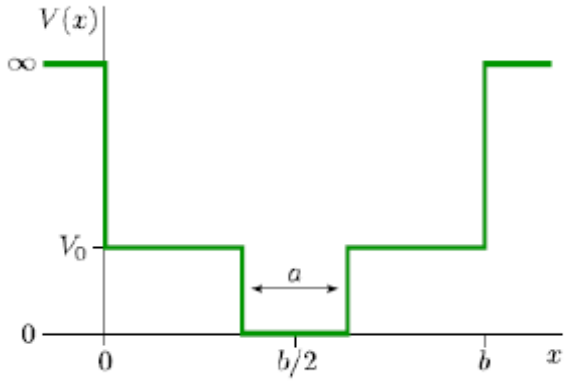

Figure 5: Potential energy function of finite well of width, a, and depth, V0, centered in an infinite well of width, b. (Schroeder, 2022).

This comes from the fact that the wavefunction is not normalized for any energy value (McQuarrie, et.al, 1997). To find the allowed energy values, we can guess different values until we get the tail of the wavefunction to exponentially decay to 0 outside of the potential well. This is known as the shooting method and we find that E ≈ 3.413571 for the first energy state as shown below. Note how now the wave function follows the boundary conditions stated for the analytical solution, smoothly decaying at the ends of the potential well and corresponding to the ground state wavefunction (0 nodes).

This method is quite literally taking shots in the dark which is not viable for scalability. We need to develop a more robust method which leads us to matrix diagonalization technique adapted from Schroeder. We know that the wavefunction is a linear combination of basis functions, ϕ_n, as shown below.

$$\psi = \sum c_n \phi_n$$

Where we need to find the coefficients, cn. A good approximation for the wavefunctions are sinusoids as analytically derived for the infinite square well problem shown below (McQuarrie, et.al, 1997).

$$\phi_n(x) = \sqrt{\frac{2}{b}} \sin\left(\frac{n\pi x}{b}\right)$$

We can now substitute in Eqn. 16 into Eqn. 2.

$$\sum H c_n \phi_n = \sum E c_n \phi_n$$

Next, we can some math tricks to obtain the matrix element Hmn as shown by below.

$$\int \phi_m^* \sum H c_n \phi_n \, dx = \int \phi_m^* \sum E c_n \phi_n \, dx$$

$$\sum \left(\int \phi_m^* H \phi_n \, dx \right) c_n = E c_m$$

$$H_{mn} = \int \psi_m^* H \psi_n \, dx$$

$$\sum H_{mn} c_n = E c_m$$

Where we define the equation above and its variables in matrix form below.

$$\begin{pmatrix} H_{11} & \cdots & H_{1n} \\ \vdots & \ddots & \vdots \\ H_{m1} & \cdots & H_{mn} \end{pmatrix} \begin{pmatrix} c_1 \\ c_2 \\ \vdots \end{pmatrix} = E \begin{pmatrix} c_1 \\ c_2 \\ \vdots \end{pmatrix}$$

$$H = H_0 + \Delta V(x)$$

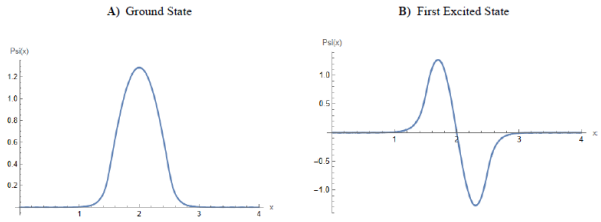

Figure 6: Corrected wavefunction plotted as a function of position for the A) ground state and B) first excited state.

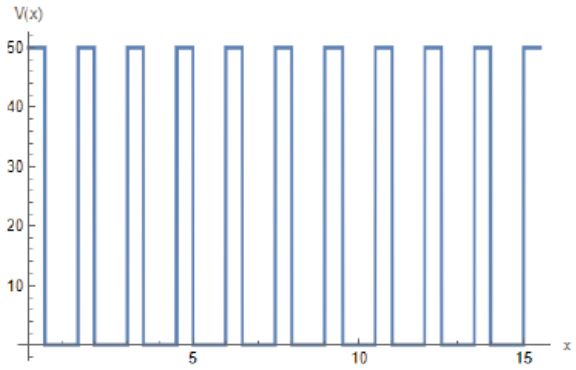

Figure 7: 10 repeating finite potential wells plotted as a function of position.

$$H_{mn} = \int \psi_m^* H_0 \psi_n \, dx + \int \psi_m^* V(x) \psi_n \, dx$$

$$= E_n \delta_{mn} + \int \psi_m^* V(x) \psi_n \, dx$$

$$E_n = \frac{n^2 \pi^2}{2mb^2}$$

Where the equation above corresponds to the energy solutions for the infinite potential well (McQuarrie, et.al, 1997). Hmn matrix elements are calculated for b = 4, a = 1, and V0 = 50 with the final tridiagonal matrix (corresponding to Eqn. 22) calculated using Mathematica's Eigensystem[] function. Before plotting the final solution, we convert the eigenvectors to their true form by using the following equation.

$$\psi = \sum c_n \phi_n$$

Notice how the shape of the objective function is identical to that calculated using the shooting method. This is corroborated by the fact that the eigenvalue (corresponding to E) for this ground state is 3.41566 which is nearly identical to 3.413571 (for shooting method). Lastly, the effectiveness of this method is shown by plotting the first excited state as shown by Figure 6B. The wavefunction looks as we expect it to with one node and exponential decay at the potential well boundaries. Note that for the shooting method, we would have to recalculate E for this state but for the matrix method all of the data is computed during the solving step. For all of these reasons, we will move forward using this diagonalization method for further calculations.

3 Multiple Finite Potential Wells

Now that we have solved simpler systems, we seek to scale our approach to multiple finite potential wells. First, we define our potential as the same as the single potential well but repeated for 10 wells. A neat trick we can do is create a pattern by using the modulus operator for the current position and the well width. This takes the fractional quotient between the two. Because this is predictably less than 1 in the desired potential well region, we can use this to define multiple wells of a given width (Schroeder, 2022).

We can then solve this potential just as before and plot the probability density, $|\phi_n|$, corresponding to the first 4 energy states.

The first thing we note is that the ground state looks similar to that of the single finite potential well. This is a roughly Gaussian distribution which states that the particle is statistically likely to reside near the center wells with decreasing probabilities away from the center. The first excited state is more of a bimodal distribution with particles residing near half of the distance to the centers. All of these energy

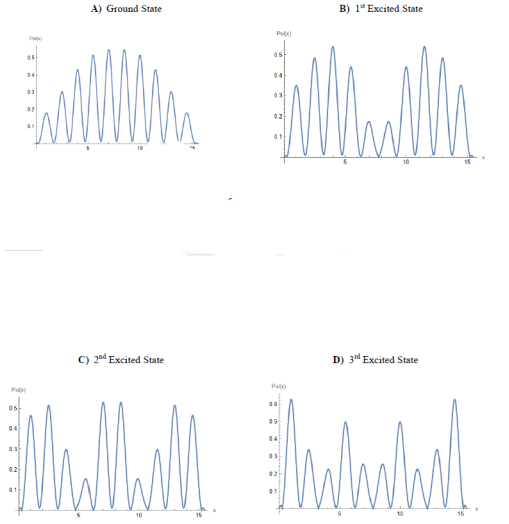

Figure 8: Corrected wavefunction plotted as a function of position for the A) ground state, B) first excited state, C) second excited state, and D) third excited state.

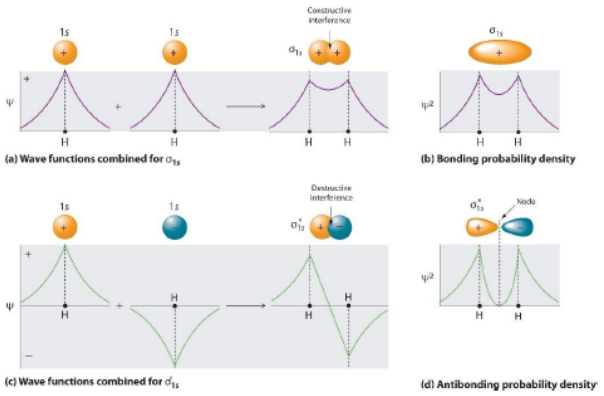

Figure 9: Schematic of wavefunctions and corresponding types of bonding orbitals (Libretext, 2022).

states can be interpreted as constructive and destructive linear combinations of atomic bonding orbitals. This is known as the LCAO molecular orbital theory.

In solids with numerous finite potential wells, atomic orbitals hybridize to form molecular orbitals with varying energies. Due to the proximity of many atoms, these orbitals create continuous energy bands. The Pauli exclusion principle restricts each orbital to a maximum of two electrons, and the bands are filled starting from the lowest energy levels (Ashcroft, et.al, 1976). We highlight this effect by plotting the energies associated with each of these linear combinations as shown below.

Note how the energy states in the 10 potential well system are so close that they start to form the characteristic bands of electrons in solids.

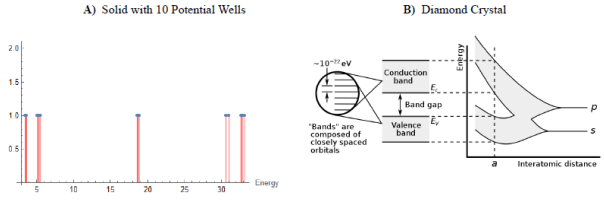

Figure 10: A) Energies associated with the 10 finite potential well system plotted and B) Example of band formation when a large number of carbon atoms are brought together to form a diamond crystal (Chetvorno, 2017).

4 Conclusion

In this paper, we successfully review the numerical and analytical solutions of the TISE for the single and multi-finite quantum potential well system.

We find results that correspond with literature calculations for both systems. Furthermore, we trace the collapse of energy states to LCAO molecular orbital theory and band structure theory. It turns out that the LCAO approach combined with these multi-finite potential wells can be utilized by computational chemists for low cost, semi empirical calculations of material electronic properties like band structure. This is especially important for systems with greater than 10,000 atoms which cannot use density functional theory (DFT) to account for complete interactions. For smaller systems however, LCAO is not very accurate as the potentials are not really a rectangular well shape but rather asymmetric like the Lennard-Jones or Morse potentials. Nevertheless, it was an important stepping stone for more accurate and widely used methods first-principles method like DFT which approximate single-particle energies (Roy, 2015).

If this were to be done in the future, maybe better generalizations for periodic potential behavior can be made such as Bloch theorem. Second, different electronic potentials like Lennard-Jones/Morse can be explored to evaluate the effect they have on results. Lastly, more computationally efficient techniques can be utilized for solvers such as the Thomas algorithm for the sparse, tridiagonal matrix and domain decomposition methods for boundary value partial differential equation (PDE) problems. The PDEs and matrix problems were found to take a lot of time solve and scaled poorly especially for the multi-finite potential well system. Making the suggested improvements may lead to new conclusions and solidify results.

5 Sources

The link to the annotated Mathematica notebook in which all calculations and plots were generated is available for download via this link

References

[1] UCSD. *Finite Square Well*. Available online: `https://courses.physics.ucsd.edu/2017/Spring/physics4e/finitesquarewell.pdf` (accessed on 2024-04-27).

[2] Vetterling, W. T. *Numerical Recipes*; Cambridge University Press, 1998.

[3] McQuarrie, D. A.; Simon, J. D. *Physical Chemistry: A Molecular Approach*; University Science Books, 1997.

[4] Schroeder, D. *Quantum Mechanics*. Available online: `https://physics.weber.edu/schroeder/quantum/QuantumBook.pdf` (accessed on 2024-04-27).

[5] Libretexts. *3.1: Molecular Orbital Theory*. Available online: `https://chem.libretexts.org/Courses/University_of_Alberta_Augustana_Campus/AUCHE_230_-_Structure_and_Bonding/03%3A_Molecular_Orbital_Theory/3.01%3A_Molecular_Orbital_Theory` (accessed on 2024-04-27).

[6] Ashcroft, N. W.; Mermin, N. D. *Solid State Physics*; Cengage, 1976.

[7] By Chetvorno - Own work, CC0, `https://commons.wikimedia.org/w/index.php?curid=56983339`

[8] Roy. *Tight Binding*. Available online: `https://www.physics.rutgers.edu/~eandrei/chengdu/reading/tight-binding.pdf` (accessed on 2024-04-27).

[9] *2.1.4 Periodic Potentials*. Available online: `https://www.tf.uni-kiel.de/matwis/amat/semi_en/kap_2/backbone/r2_1_4.html` (accessed on 2024-04-27).